

Nanostructure and Magnetic Field Ordering in Aqueous Fe₃O₄ Ferrofluids: A Small-Angle Neutron Scattering Study

A. Taufiq^{1*}, Sunaryono¹, N. Hidayat¹, E.G.R. Putra², A. Okazawa³, I. Watanabe⁴, N. Kojima⁵, S. Pratapa⁶ and D. Darminto⁶

¹Department of Physics, Faculty of Mathematics and Natural Sciences, Universitas Negeri Malang, 65145 Malang, Indonesia

²Sekolah Tinggi Teknologi Nuklir, National Nuclear Energy Agency of Indonesia, 55281 Yogyakarta, Indonesia

³Department of Basic Science, The University of Tokyo, Komaba, Meguro-ku, 153-8902 Tokyo, Japan

⁴Advanced Meson Science Laboratory, Nishina Center, RIKEN, 2-1, Hirosawa, Wako, 351-0198 Saitama, Japan

⁵Toyota Physical and Chemical Research Institute, Yokomichi 41-1, Nagakute, 480-1192 Aichi, Japan

⁶Department of Physics, Faculty of Science, Institut Teknologi Sepuluh Nopember, 60111 Surabaya, Indonesia

ARTICLE INFO

Article history:

Received 11 September 2017

Received in revised form 2 August 2019

Accepted 2 August 2019

Keywords:

Ferrofluid

Fe₃O₄

SANS

Nanostructure

Ordering

Superparamagnetic

ABSTRACT

Despite the importance of reducing production costs, investigating the hierarchical nanostructure and magnetic field ordering of Fe₃O₄ ferrofluids is also important to improve its application performance. Therefore, we proposed an inexpensive synthesis method in producing the Fe₃O₄ ferrofluids and investigated their detailed nanostructure as the effect of liquid carrier composition as well as their magnetic field ordering. In the present work, the Fe₃O₄ ferrofluids were successfully prepared through a coprecipitation route using a central precursor of natural Fe₃O₄ from iron sand. The nanostructural behaviors of the Fe₃O₄ ferrofluids, as the effects of the dilution of the Fe₃O₄ particles with H₂O as a carrier liquid, were examined using a small-angle neutron spectrometer (SANS). The Fe₃O₄ nanopowders were also prepared for comparison. A single lognormal spherical distribution and a mass fractal model were applied to fit the neutron scattering data of the Fe₃O₄ ferrofluids. The increasing carrier liquid composition of the fluids during dilution process was able to reduce the fractal dimension and led to a shorter length of aggregation chains. However, it did not change the size of the primary particles or building block (approximately 3.8 nm) of the Fe₃O₄ particles. The neutron scattering of the Fe₃O₄ ferrofluids under an external magnetic field in the range of 0 to 1 T exhibited in a standard way of anisotropic phenomenon originating from the nanostructural ordering of the Fe₃O₄ particles. On the other hand, the Fe₃O₄ powders did not show anisotropic scattering under an external field in the same range. Furthermore, the magnetization curve of the Fe₃O₄ ferrofluids and nanopowders exhibited a proper superparamagnetic character at room temperature with the respective saturation magnetization of 4.4 emu/g and 34.7 emu/g.

© 2019 Atom Indonesia. All rights reserved

INTRODUCTION

In recent years, Fe₃O₄ nanoparticles have grown-up to become more exciting materials due to their applications in many fields. During the last five years, many researchers have reported that Fe₃O₄ nanoparticles especially in ferrofluids, can be applied as a ligand for biocatalyst [1], a dopamine content identifier [2],

a circulating tumor cells detector [3], a printer of microstructures in a polymer matrix [4], a heat transfer enhancement in heating and cooling system [5], an antibacterial and hyperthermia [6], a catalyst [7], a material for spintronic device [8], a sorbent for removal of oil from wastewater [9], an enhancer for catalytic reaction and drug delivery [10], an electromagnetic wave absorber [11], an enhancer for a catalytic reduction of 4-nitrophenol [12], a DNA-bases determiner [13], an adsorbent in wastewater treatment [14], and a catechol biosensor [15].

*Corresponding author.

E-mail address: ahmad.taufiq.fmipa@um.ac.id

DOI: <https://doi.org/10.17146/aij.2019.744>

Numerous synthesis methods have been carried out to prepare Fe_3O_4 nanoparticles in various sizes, forms, and distributions. Related to the preparation of the Fe_3O_4 ferrofluids, one of the primary targets in synthesizing Fe_3O_4 nanoparticles is obtaining the particles in nanometric size with a proper distribution in a single-domain character. The synthesis methods that have been trusted in attaining the target are, for example, coprecipitation [16], decomposition of homemade iron oleate [17], microemulsion-solvothermal [18], microwave-solvothermal [19], hydrothermal [20], sol gel-hydrothermal [21], ultrasonic irradiation [22], static magnetic field-assisted [23] and mechano-chemistry [24]. However, such methods tend to be costly because of their expensive raw materials as primary precursors. Therefore, in this work, we propose an alternative approach by using an inexpensive primary precursor of iron sand obtained from natural Indonesian resource.

Fe_3O_4 ferrofluids or magnetic colloids are composed of single-domain magnetite particles dispersing in an appropriate liquid carrier [25]. Previous papers showed that ferrofluids tend to be unstable fluids due to agglomeration phenomena [26-28]. In order to obtain stable Fe_3O_4 ferrofluids, the Fe_3O_4 nanoparticles can be coated with a surfactant such as tetra methyl ammonium hydroxides (TMAH). Furthermore, the liquid carrier composition of the ferrofluids also plays an essential role in keeping the stabilization of the fluids. In previous work, it was shown that the composition of water as a liquid carrier could reduce the size of the fractal aggregation of Fe_3O_4 ferrofluids from about 3 to 2 dimension, as studied by SANS [29]. However, a stable ferrofluid without any aggregation is still very difficult to be appropriately obtained. For that reason, to acquire stable Fe_3O_4 ferrofluids in the absence of fractal structure, we investigate the effects of variations in the compositions of Fe_3O_4 particles and liquid carrier on nanostructures of fluids.

Despite the effects of variations in compositions, the structures of the fluids were also strongly affected by an external magnetic field. Nkurikiyimfura and co-workers reported that external magnetic field induces the nanostructural-ordering such as the chain-like structures of Fe_3O_4 particles in ferrofluids [30]. They successfully showed that the ferrofluids with nanostructural ordering in extended chain-like structures significantly increase their thermal conductivity under an external magnetic field. However, regarding nanostructural ordering, they only predicted the effect of magnetic field on the

nanostructures by modeling analysis without experimental data. Therefore, in order to deepen the detailed structures, in place of exploring the structural stability of the fluids due to particle concentration, we also present our investigation on the nanostructural ordering of both Fe_3O_4 fluids and powders based on such magnetic field by conducting a SANS experiment. SANS was employed to examine the structures directly, and also the nanostructural ordering of the Fe_3O_4 in the fluids and powders under external magnetic field. Moreover, the magnetization and superparamagnetic characters of the Fe_3O_4 powders and ferrofluids are also discussed.

EXPERIMENTAL METHODS

As the starting material, the iron sand originated from Indonesia was used to prepare the Fe_3O_4 powders and ferrofluids by employing a coprecipitation method. The analytical grade of hydrochloric acid (HCl) and ammonium hydroxide (NH_4OH) from Sigma-Aldrich were used as dissolving and precipitating agents in preparing the Fe_3O_4 particles. Furthermore, the analytical grades of TMAH from Sigma-Aldrich and H_2O were also employed as a surfactant and dispersing agents respectively, to make stable Fe_3O_4 ferrofluids. The details of the experimental procedure for producing Fe_3O_4 powders and ferrofluids were reported in our previous works [31-33]. Finally, the dilution of Fe_3O_4 ferrofluids with liquid carrier specified by volume composition of H_2O and Fe_3O_4 ferrofluids were 0:1, 1:1, 1:2 and 1:5 respectively.

The crystal structure, phase purity, and functional groups of the Fe_3O_4 particles were investigated using X-ray diffractometer (XRD) and Fourier transform infra-red (FTIR) spectrometer at room temperature, respectively. The specific nanostructural properties of the Fe_3O_4 powders and ferrofluids were investigated in BATAN Indonesia using a 36-meter SANS spectrometer. During the SANS experiment, the nanostructural ordering was studied by maintaining an external field of 1 T. After conducting the SANS experiment, the scattering intensities of the samples were then subtracted to be analyzed. For data analysis, we applied a single lognormal spherical distribution and a mass fractal model in fitting the neutron scattering data. Furthermore, the magnetic properties of the Fe_3O_4 powders and fluids were examined using SQUID magnetometer at The University of Tokyo, Japan. A magnetic field ranging from -5 to 5 T was applied to obtain the hysteresis curve of the Fe_3O_4 powders and fluids.

RESULTS AND DISCUSSION

In order to investigate the crystal structure and phase purity of the Fe₃O₄ particles, the X-ray diffraction experiment was engaged to obtain the diffraction patterns as shown in Fig. 1. Based on the fitting analysis (represented by solid line) of the experimental data using Rietveld analysis, it was found that the Fe₃O₄ particles constructed a single phase in a cubic structure with the space group of *Fd-3mZ*. From the quantitative analysis, the lattice parameters and goodness of fit were $a = b = c = 8.362 \text{ \AA}$ and 0.701, respectively. In such space group, the Fe²⁺ and Fe³⁺ ions randomly occupied octahedral and tetrahedral positions [34]. The Fe ions in tetrahedral positions occupied a tetrahedron position surrounded by four oxygen atoms. Meanwhile, the Fe ions in octahedral positions occupied an octahedron position surrounded by six oxygen atoms.

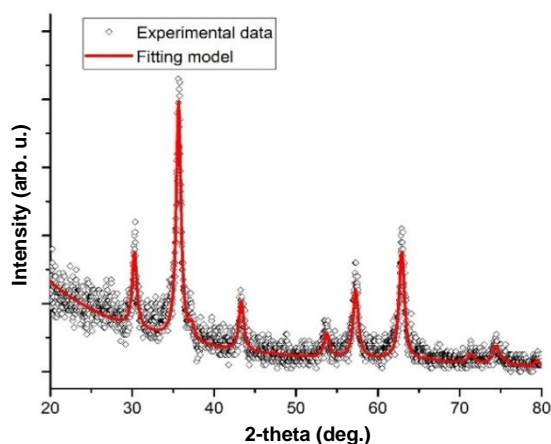


Fig. 1. XRD data and fitting model of the Fe₃O₄ particles.

For the certainty that the Fe ions occupied the sites, we investigated the functional groups of the prepared Fe₃O₄ particles at a wavenumber in the range of 400 - 3500 cm⁻¹. The data analysis of the FTIR spectra as shown in Fig. 2 exhibited that the functional groups of the Fe-O, both in tetrahedral and octahedral sites were determined at the wavenumber of ~580 and ~1540 cm⁻¹. Meanwhile, the peaks at the wavenumbers of ~1635 and ~3340 cm⁻¹ were originated from the functional groups of respective hydroxyl groups and bands of water [35]. Such data provides information that the Fe ions consisting of Fe²⁺ and Fe³⁺ are randomly placed in the spinel system, which corresponds to the X-ray diffraction data. In line with the FTIR data, the previous work presented that the Fe₃O₄ particles formed a single phase in a spinel cubic structure [31,36].

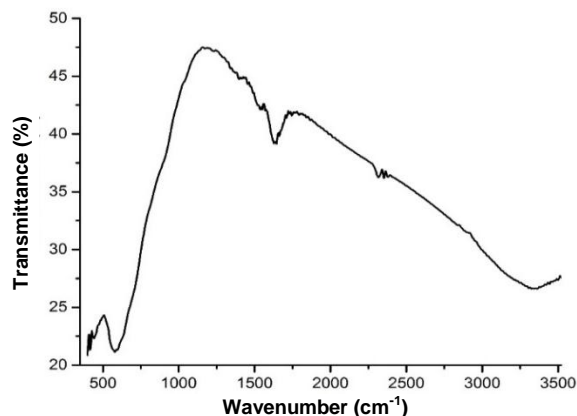


Fig 2. FTIR spectrum of the Fe₃O₄ particles.

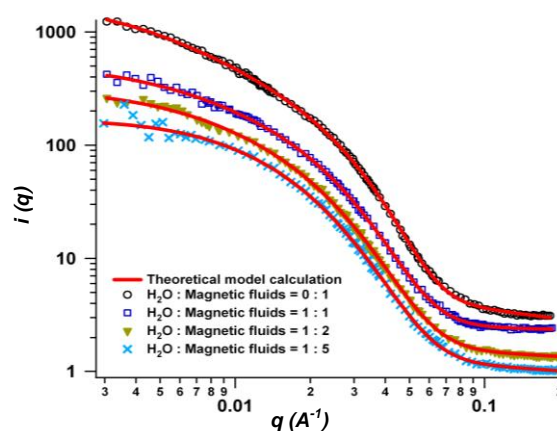


Fig. 3. SANS profiles of the Fe₃O₄ ferrofluids.

Figure 3 and table 1 present SANS profiles of the samples and their data analysis results. The figure gives information on the scattering intensity (i) and momentum transfer as scattering vector (q). In this work, a lognormal distribution model as a form factor was employed to determine the distribution and size of the Fe₃O₄ particles according to Equation 1 [28].

$$P(R) = \frac{1}{R\sigma\sqrt{2\pi}} \exp\left(-\frac{\ln^2\left(\frac{R}{R_0}\right)}{2\sigma^2}\right) \quad (1)$$

Where σ refers to the standard deviation and R_0 refers to the characteristic radius of the distribution. Meanwhile, the mass fractal structure [37] of the Fe₃O₄ particles as a structure factor was explored according to Equation 2.

$$S(q) = 1 + \frac{D\Gamma(D-1)}{(D-1)/2} \times \sin[D-1] \tan^{-1}(q\xi) \times (qR)^D \left[1 + \frac{1}{(q^2\xi)^2} \right] \quad (2)$$

Where S is the structure factor, q is the scattering vector, D is the fractal dimension, R is the size of particles in a spherical form, and ξ is the correlation length.

The SANS data were fitted by employing the two-lognormal spherical model to calculate the primary (R_1) and secondary particles (R_2) as clusters. A single mass fractal model was combined to calculate the structure factor (S). In this case, Equation 3 presents the theoretical model for global fitting [32].

$$i(q) \approx \int_0^\infty N_1(R_1)F_N^2(q, R_1)dR_1 + \int_0^\infty N_2(R_2)F_N^2(q, R_2)dR_2 S(q, \xi, D, R_2) \quad (3)$$

where i refers to the scattering intensity, F refers to the scattering amplitude, and N refers to the number density of the particles.

Based on Fig. 3, it is evident that all SANS patterns of the Fe₃O₄ ferrofluids have a similar trend at medium and high q values, but a different trend at low q . The figure represents that the size of the Fe₃O₄ primary particles in the fluids was stable and not affected by the variations of liquid carrier contents. The increasing liquid carrier content only contributed to reducing the fractal dimension that can be easily seen by lowering the slope of the scattering patterns at the low- q regime. However, a quantitative analysis by using a global fitting [32], is necessary to calculate the primary particles and fractal structure of the Fe₃O₄ ferrofluids in exact values. The SANS patterns of the Fe₃O₄ ferrofluids were firstly fitted using Eq. 3. On the other hand, the fitting model was not appropriate with the SANS data, which implied that the Fe₃O₄ nanoparticles in the fluids have different structures from the powders. Consequently, we propose another model for fitting the SANS data using a single lognormal and a mass fractal model without adding the secondary particles. The following equation presents the mathematical model.

$$i(q) \approx \int_0^\infty N_1(R_1)F_N^2(q, R_1)dR_1 S(q, \xi, D, R_1) \quad (4)$$

It is clear that the experimental data of SANS (represented by circles, squares, triangles, and cross symbols) coincide with the theoretical model calculation (represented by a solid line). Table 1 shows the fitting results of the SANS data of the fluids diluted with water as a liquid carrier in several compositions using Eq. 4. The table points out that the size of the Fe₃O₄ primary particles (R_1) in the fluids did not change due to the liquid carrier

compositions. The primary particles of the Fe₃O₄ in the fluids were formed during the precipitation process before the addition of the of TMAH surfactant. The surfactant was not able to reduce the size of the building block, but effectively covered the surface of the Fe₃O₄ particles in order to enhance the fluid stabilization by reducing the size of clusters or aggregations. The size of fractal aggregate (ξ) is decreased by increasing the liquid carrier content. It reveals that the dilution of the Fe₃O₄ ferrofluids by increasing water content leads to a shorter length of aggregation chains. The reduction of aggregation chains occurred in dilution process by giving mechanical energy such as kinetic energy from the magnetic bar at 1000 rpm during the synthesis process. After covering the surface of the Fe₃O₄ primary particles in the fluids, TMAH continuously prevented aggregations of the particles. Therefore, the high-speed rotation of the magnetic bar during the stirring process is believed to break aggregates of the Fe₃O₄ particles in the fluids.

Table 1. Fitting results of the SANS data for the Fe₃O₄ ferrofluids

Sample	R_1 (nm)	R_2 (nm)	ξ (nm)	D
H ₂ O : Fe ₃ O ₄ ferrofluids = 0:1	3.8	-	45.3	1.2
H ₂ O : Fe ₃ O ₄ ferrofluids = 1:1	3.8	-	27.8	1.1
H ₂ O : Fe ₃ O ₄ ferrofluids = 2:1	3.8	-	23.4	1.1
H ₂ O : Fe ₃ O ₄ ferrofluids = 5:1	3.8	-	-	-
Fe ₃ O ₄ nanopowders [32]	3.8	9.3	-	2.9

Different with the Fe₃O₄ particles in the fluids, the Fe₃O₄ powders have similar primary particles (R_1) of approximately 3.8 nm, which constructed bigger particles (R_2) as secondary particles or clusters of about 9.3 nm with a fractal dimension (D) = 2.9. It means that the primary particles of Fe₃O₄ powders as building block construct clusters in a large size and grow up in 3-dimensional structures as aggregations. Theoretically, the smaller the particles size of the Fe₃O₄ nanoparticles, the larger their affinity to form aggregates relating to low energy barriers [38]. Moreover, the interparticle interactions of the magnetic nanoparticles also play an essential role in the aggregation process. It means that the Fe₃O₄ powders have similar primary particles with the magnetic fluids [31,32]. However, the Fe₃O₄ powders constructed bigger particles as clusters or secondary particles with a higher fractal dimension than magnetic fluids. These results become physical evidence that employment of TMAH as a surfactant is already successful to cover the surface of magnetic particles in preventing the agglomeration growth.

The fitting results also provide further information on the fractal dimension (D). In general, the D value of the Fe_3O_4 ferrofluids reduced from about 1.2 to 1.1 and then disappeared at the highest liquid carrier content. The fractal dimension value which is close to 1 can be associated with the chain-like structures. The increasing liquid carrier content in the Fe_3O_4 ferrofluids has a consequence of an expansion of dilution volume, i.e., a significant distance among magnetic nanoparticles that yields small interactions among magnetic particles. The lower the liquid carrier content, the higher the concentration of the magnetic nanoparticles gaining domination of the interparticle correlation interference [29]. Furthermore, at the highest liquid carrier content, the fitting analysis points out that the fractal dimension of the sample has a probable value that is lower than 1, which is associated with the absence of the fractal structure. The absence of the fractal structure $S(q) \sim 1$, is a consequence of the scattering that only contributed to the form factor. This phenomenon guides us to the estimated conclusion that the composition of ferrofluids and the liquid carrier has a critical value to break the fractal structure. Thus, each sample has different aggregation structures caused by the increasing liquid carrier content during the dilution process. The mean distances among Fe_3O_4 nanoparticles in the fluids become increasingly distant. The higher the liquid carrier content, the longer the distance between magnetic particles in the fluids. At the critical value, the magnetic particles can be determined by isolated particles. Consequently, the scattering is only contributed by the form factor without any interference from the structural factor (fractal structure). As a result, the Fe_3O_4 ferrofluids with the highest liquid carrier composition have proper criteria as stable fluids that open a high potential to be applied in many fields. In this stage, the given kinetic energy can impair fractal structure stability of the Fe_3O_4 ferrofluids. Theoretically, the mechanism of aggregations contributes to construct fractal dimension. Furthermore, the balance between repulsive and attractive interactions, and the thermal contribution contribute to the instability of the Fe_3O_4 ferrofluids [39]. Regardless of investigations of the contribution of liquid carrier to reduce fractal structures, further SANS experiments by applying an external magnetic field of both Fe_3O_4 powders and ferrofluids were also carried out to examine the nanostructural ordering.

Based on Fig. 4, the scattering of the Fe_3O_4 powders has similar isotropic patterns with the Fe_3O_4 ferrofluids without an external magnetic field. Interestingly, under a magnetic induction of 1 T during SANS experiment, the Fe_3O_4 ferrofluids exhibit anisotropic scattering, but it does not appear

on the Fe_3O_4 powders. Based on Fig. 6, it is clear that under the external field of 1 T, the magnetic moments of the Fe_3O_4 particles both in powders and fluids are parallel to the direction of the external field and they tend to saturate. However, the neutron scatterings of the Fe_3O_4 in powders and fluids under a magnetic induction of 1 T are different. Therefore, we suppose that the anisotropic neutron scattering in the fluids could be contributed by the nanostructural ordering of the Fe_3O_4 particles originating from the natural orientation of the particles influenced by the magnetic field. Moreover, the flexibility of the liquids also contributes to the particles ordering of the Fe_3O_4 . On the other hand, the magnetic particles are difficult to orientate in the powders because their particles have a low degree of flexibility of motion. Under an external field, the particles in the fluids orientate easily following the Brownian motion. Fig. 5 and Fig. 6 visualize the structures of the Fe_3O_4 powders and ferrofluids without and with a magnetic induction of 1 T.

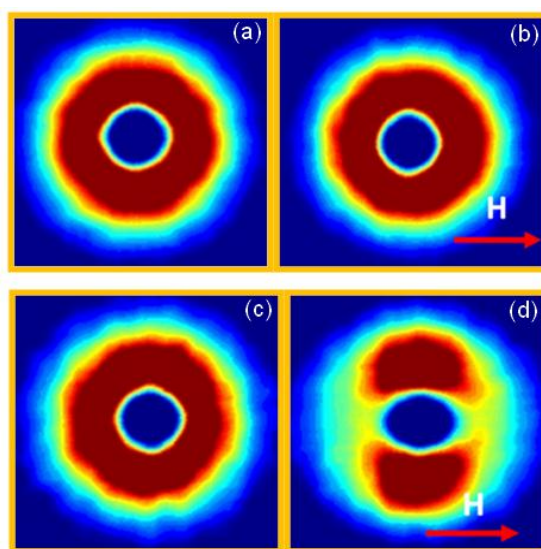


Fig. 4. SANS profiles of the Fe_3O_4 powders (a) without and with (b) the external field of 1 T, the Fe_3O_4 ferrofluids (c) without and with (d) external field of 1 T.

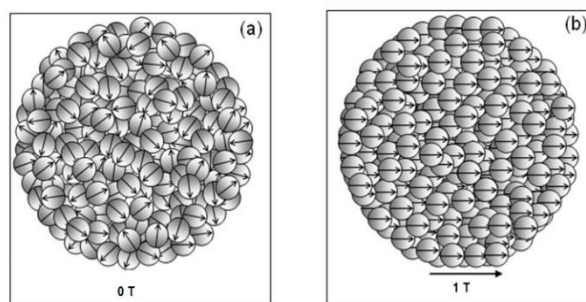


Fig 5. Structural models of the Fe_3O_4 powders (a) without and (b) with an external field 1 T.

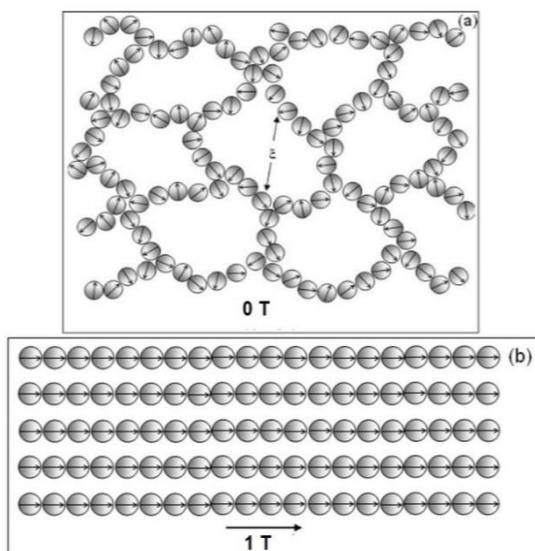


Fig. 6. Structural models of the Fe_3O_4 ferrofluids (a) without and (b) with the external field.

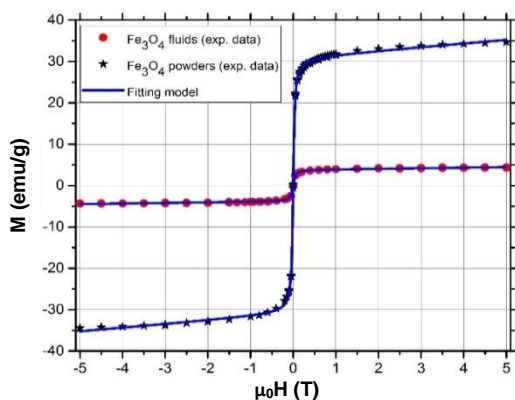


Fig. 7. M-H curves of the Fe_3O_4 nanopowders and ferrofluids.

Based on Fig. 5 (a), the Fe_3O_4 powders aggregate in compact structures (3-dimensional structures) that represent the fractal dimension (D) = 2.9 calculated from the mathematical model. Without external field, the magnetic moments have a random orientation. On the other hand, under the external field of 1 T as displayed in Fig. 5(b), the magnetic moments of the Fe_3O_4 particles are oriented by following the magnetic field direction. However, the magnetic particles are difficult to be oriented because the particles are constrained in their solid state. The structural model of magnetic particles orientation in this work is also appropriate with the model proposed by another group [40]. Furthermore, in the absence of an external magnetic field as displayed in Fig. 6(a), the Fe_3O_4 particles in the fluids with chain-like structures are forced to be oriented in producing structural ordering as visualized in Fig. 4(d). Under a magnetic induction of 1 T as shown in Fig. 6(b), the magnetic particles in the fluids orientate easily following the magnetic moment's orientation. The magnetic particles in the

fluids then formed a long structural ordering in 1 dimension. In good agreement with this work, Nkurikiyimfura *et al.* proposed a structural orientation model of magnetic particles in extended chain-like structures under the effect of an external field [30]. Moreover, Mehta *et al.* also reported that by employing an external field during SANS experiment, the particles changed their structures and built long-range orders of chains [27].

Despite studying the nanostructural properties, studying the magnetic properties of the Fe_3O_4 ferrofluids also become important. The magnetic properties of the Fe_3O_4 in powders and fluids investigated by using a SQUID magnetometer is presented in Fig. 7. The figure shows the M-H are fitted properly by Langevin function. The solid star, circle, and solid line represent the experimental data of the Fe_3O_4 nanopowders and ferrofluids, and fitting model using Langevin function, respectively. Based on the fitting analysis, the Fe_3O_4 in powders and fluids have coercivity value of approximately 0 with S-shape indicating a superparamagnetic character [41-43]. The saturation magnetization value of the Fe_3O_4 in powders and fluids are 34.7 and 4.4 emu/g, respectively. The increasing saturation magnetization of the Fe_3O_4 powders originated from the secondary particles as clusters, aggregation, and fractal dimension. Theoretically, in the absence of an external field, the magnetic moments of the superparamagnetic material have a random orientation and they orientate in the direction of the magnetic field under an external field. In the fluids, the random orientation of the magnetic single-domain particles is contributed by the thermal energy overcoming the anisotropy energy barrier [44].

CONCLUSION

The Fe_3O_4 ferrofluids were successfully prepared using local natural iron-sand. The increasing liquid carrier content in the Fe_3O_4 ferrofluids was able to reduce the aggregation chains and fractal dimension. Meanwhile, the size of the Fe_3O_4 primary particles of approximately 3.8 nm was not changed by different liquid carrier compositions. Interestingly, under an external field of 1 T, the neutron scattering of the fluids exhibited an anisotropic pattern corresponding to the nanostructural ordering of the Fe_3O_4 particles. However, the anisotropic pattern of the Fe_3O_4 powders was not observed. Furthermore, the magnetization curve of the Fe_3O_4 nanopowders and ferrofluids displayed a superparamagnetic character.

ACKNOWLEDGMENT

We would like to thank the Central Laboratory of Universitas Negeri Malang, Malang-Indonesia; the Neutron Scattering Laboratory at BATAN, Serpong-Indonesia; and the University of Tokyo, Tokyo-Japan; for the facilities of sample preparations and characterizations. This work is partially supported by the research grant from KEMENRISTEKDIKTI RI for AT.

REFERENCES

- M. Abbaszadeh and P. Hejazi, *Food Chem.* **290** (2019) 47.
- A. Thamilselvan, P. Manivel, V. Rajagopal *et al.*, *Colloids Surf. B Biointerfaces* **180** (2019) 1.
- Z.H. Sun, L.H. Zhou, G.J. Deng *et al.*, *Chin. J. Anal. Chem.* **45** (2017) 1427.
- A.R.A. Fattah, S. Ghosh and I.K. Puri, *J. Magn. Magn. Mater.* **401** (2016) 1054.
- D. Toghraie, S.M. Alempour and M. Afrand, *J. Magn. Magn. Mater.* **417** (2016) 243.
- N.T. Nguyen, D.L. Tran, D.C. Nguyen *et al.*, *Curr. Appl. Phys.* **15** (2015) 1482.
- T. Yao, Q. Zuo, H. Wang *et al.*, *J. Colloid Interface Sci.* **450** (2015) 366.
- A.M. Noval, J.R. Zuazo, E.S. Colera *et al.*, *Appl. Surf. Sci.* **355** (2015) 698.
- L. Yu, G. Hao, J. Gu *et al.*, *J. Magn. Magn. Mater.* **394** (2015) 14.
- W. Zhang, X. Si, B. Liu *et al.*, *J. Colloid Interface Sci.* **456** (2015) 145.
- T.Y. Wu, K.T. Lu, C.H. Peng *et al.*, *Mater. Res. Bull.* **70** (2015) 486.
- F. Yan and R. Sun, *Mater. Res. Bull.* **57** (2014) 293.
- B. Kaur and R. Srivastava, *Colloids Surf. B Biointerfaces* **118** (2014) 179.
- M. Khatamian, B. Divband and R. Shahi, *J. Water Process Eng.* **31** (2019) 1.
- C. Karami and M.A. Taher, *Int. J. Biol. Macromol.* **129** (2019) 84.
- S. Rani and G.D. Varma, *Phys. B Condens. Matter* **472** (2015) 66.
- F. Jiang, X. Li, Y. Zhu *et al.*, *Phys. B Condens. Matter* **443** (2014) 1.
- Y. Li, R. Jiang, T. Liu *et al.*, *Ceram. Int.* **40** (2014) 1059.
- A.A. Hernández-Hernández, G.A. Álvarez-Romero, A. Castañeda-Ovando *et al.*, *Mater. Chem. Phys.* **205** (2018) 113.
- X.-D. Liu, H. Chen, S.-S. Liu *et al.*, *Mater. Res. Bull.* **62** (2015) 217.
- P. Lorkit, M. Panapoy and B. Ksapabutr, *Energy Procedia* **56** (2014) 466.
- R. Abazari, A.R. Mahjoub, S. Molaie *et al.*, *Ultrason. Sonochem.* **43** (2018) 248.
- Y. Liu, J. Bai, H. Duan *et al.*, *Chin. J. Chem. Eng.* **25** (2017) 32.
- B. Medina, M.G.V. Fressati, J.M. Gonçalves *et al.*, *Mater. Chem. Phys.* **226** (2019) 318.
- M.A. Baqiya, A. Taufiq, Sunaryono *et al.*, *Spinel - Structured Nanoparticles for Magnetic and Mechanical Applications*, in: *Magnetic Spinels - Synthesis, Properties and Application*, InTech, Croatia (2017) 253. doi: 10.5772/66293
- J. Li, X. Qiu, Y. Lin *et al.*, *Appl. Surf. Sci.* **256** (2010) 6977.
- R.V. Mehta, P.S. Goyal, B.A. Dasannacharya *et al.*, *J. Magn. Magn. Mat.* **149** (1995) 47.
- F.L.O. Paula, R. Aquino, G.J. da Silva *et al.*, *J. Appl. Crystallogr.* **40** (2007) s269.
- E.G.R. Putra, B.S. Seong, E. Shin *et al.*, *J. Phys. Conf. Ser.* **247** (2010) 1.
- I. Nkurikiyimfura, Y. Wang and Z. Pan, *Exp. Therm. Fluid Sci.* **44** (2013) 607.
- A. Taufiq, Sunaryono, N. Hidayat *et al.*, *Nano* **12** (2017) 1750110.
- A. Taufiq, Sunaryono, E.G.R. Putra *et al.*, *J. Supercond. Nov. Magn.* **28** (2015) 2855.
- A. Taufiq, Sunaryono, E.G.R. Putra *et al.*, *Funct. Prop. Mod. Mater.* **827** (2015) 213.
- M.N. Shetty, *Materials Science and Engineering: Problems with Solutions*, PHI Learning Private Limited, Delhi (2016).
- H. Hamad, M.A. El-Latif, A.E. Kashyout *et al.*, *New J. Chem.* **39** (2015) 3116.
- Sunaryono, A. Taufiq, N. Mufti *et al.*, *J. Inorg. Organomet. Polym. Mater.* **28** (2018) 2206.
- J. Teixeira, *J. Appl. Crystallogr.* **21** (1988) 781.

38. A.R. Petosa, D.P. Jaisi, I.R. Quevedo *et. al.*, Environ. Sci. Technol. **44** (2010) 6532.
39. S. Genc, *Heat Transfer of Ferrofluid*, in: Nanofluid Heat and Mass Transfer in Engineering Problems, M.S. Kandelousi (Ed.), InTech, Croatia (2017) 141.
doi: 10.5772/65912
40. D. Rosicka and J. Sembera, Nanoscale Res. Lett. **6** (2011) 527.
41. A. Taufiq, A.F. Muyasaroh, S. Sunaryono *et al.*, J. Magn. **23** (2018) 337.
42. W.M. Daoush, J. Nanomed. Res. **5** (2017) 1.
43. Y. Zhang, L. Zhang, X. Song *et al.*, J. Nanomater. **2015** (2015) 1.
44. V.H. Ojha and K.M. Kant, Phys. B Condens. Matter **567** (2019) 87.